A shrink-fit problem between an eccentric and a solid of hollow shaft annulus

T Videnic and **F Kosel***
Faculty of Mechanical Engineering, University of Ljubljana, Ljubljana, Slovenia

Abstract: The paper presents an analytical solution of a shrink-fit problem between an eccentric and a centric circular annulus in the elastic domain. It is assumed that the material constants for both elements are the same and that a plane stress or plane strain state occurs in both annuli. The problem is solved using complex variable functions, where conformal mapping of the centric circular annulus to the eccentric one can be used. Elements of the stress tensor and displacement vector in both annuli are written in closed and finite form.

Keywords: shrink fit, eccentric and centric circular annulus, elasticity, complex variable functions

NOTATION

a	real constant
A	real constant in mapping function ω
a_k	coefficients of the Laurent series of function $\varphi_*(\zeta)$
b_k	coefficients of the Laurent series of function $\psi_*(\zeta)$
C, C_1, C_2	complex constants
e	Neper's number
e_0	eccentricity of the shrink-fit assembly
e_1, e_{1x}, e_{1y}	position of the shrink-fit assembly (see Figs 1 to 3)
E	Young's modulus
f_1, f_2	boundary conditions on contours γ_1 and γ_2
h	width of the shrink-fit assembly
i	imaginary unit
k_1, k_2, k_3, k_4	dimensionless ratios
L, L_0, L_1, L_2	contours of the shrink-fit assembly
M_t	torque that can be borne by the shrink-fit assembly
r_0	outer radius of the inner centric member of the shrink-fit assembly
r_1	inner radius of the inner centric member of the shrink-fit assembly
r_2	outer radius of the outer non-centric member of the shrink-fit assembly
s	arc on contour L
S, S_1, S_2	domains of the shrink-fit assembly
t, t_0, t_1, t_2	coordinates on contours L, L_0, L_1, L_2
u_{nx}, u_{ny}	components of the displacement vector on contour L
u_x, u_y	components of the displacement vector
x, y	Cartesian coordinates
x_0, y_0	Cartesian coordinates on contour L_0
X_n, Y_n	components of the surface force on contour L
z	complex variable
z_0	dimensionless complex variable
α	angle (see Fig. 2)
γ_1, γ_2	inner and outer contour on the mapped domain Σ
δ	displacement jump on contour L_0
ζ	complex variable on the mapped domain Σ
η, ξ	Cartesian coordinates on the mapped domain Σ
λ_1, λ_2	coordinates on contours γ_1 and γ_2
μ	shear modulus
μ_S	static friction coefficient
ν	Poisson's ratio
π	Ludolf's number
ρ_1, ρ_2	inner and outer radius of the circular domain Σ
σ_E	Huber's effective stress
σ_n	normal stress on contact contour L_0
σ_x, σ_y, τ_{xy}	components of the stress tensor
σ_Y	yield stress
Σ	mapped domain
τ_n	shear stress on contact contour L_0
φ, φ_1, φ_2, φ_*	complex analytical functions

The MS was received on 30 December 2003 and was accepted after revision for publication on 17 June 2004.
**Corresponding author: Faculty of Mechanical Engineering, University of Ljubljana, Askerceva 6, 1000 Ljubljana, Slovenia.*
E-mail: franc.kosel@fs.uni-lj.si

χ	Kolosov's constant in plane stress
ψ , ψ_1, ψ_2, ψ_*	complex analytical functions
ω	conformal mapping function

1 INTRODUCTION

A shrink-fit assembly between two structural components, in the continuation called the inner and outer member, can be made when the inner member is stamped into the outer one. To begin with, the outer diameter of the inner member is slightly bigger than the inner diameter of the outer member for a displacement jump δ. A shrink fit can be achieved if the outer member is expanded by heating, slipped over the inner member and then allowed to cool. Such assemblies are frequently used in engineering as a simple way of torque or some other load transmission. By suitable choice of the displacement jump δ, the bearing capacity of a construction can be increased.

Shrink-fit problems between non-centric or non-circular members are very interesting for engineering, but are mathematically complicated to solve. It is possible to solve such problems in the elastic domain using the complex variable function method, where conformal mapping of an arbitrarily shaped domain to a circular domain can be used. Doing so, the boundary conditions on a circle can be satisfied much more easily. There have been quite a few papers [**1**–**5**] dealing with the mechanical behaviours of shrink-fitted joints in the elastic domain by the complex variable function method. Mainly they relate to joints between circular members or circular members imbedded in half-space.

The systematic use of complex variable theory in plane elasticity was first proposed by Kolosov [**6**], who found that the stress and displacement state in a plane elastic problem can be expressed by two complex functions $\varphi(z)$ and $\psi(z)$. A very significant contribution to the complex variable methods was proposed by Muskhelishvili [**7**], while problems with mixed boundary conditions were dealt with in detail by Sherman [**8**, **9**].

2 THEORY OF A SHRINK FIT BETWEEN NON-CIRCULAR MEMBERS

Some general theory of a shrink fit between two arbitrarily shaped members with identical elastic constants, which was proposed by Sherman [**9**], will briefly be presented. A finite twofold connected domain S consists of two elastic domains S_1 and S_2. Let the inner boundary of domain S be denoted by L_1 and the outer one by L_2. The inner domain S_1 is shrink-fitted into the outer domain S_2. While the boundaries L_1 and L_2 are of an arbitrary shape, let the contact boundary L_0 be circular (Fig. 1). In accordance with Muskhelishvili's and Sherman's theory, the problem of determining the stress and

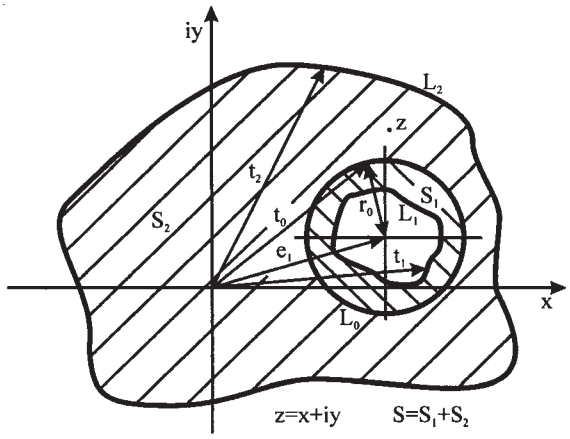

Fig. 1 Geometry of two shrink-fitted non-circular members

displacement state in both members can be solved in terms of four complex functions $\varphi_1(z)$, $\psi_1(z)$, $\varphi_2(z)$ and $\psi_2(z)$, which must be analytical in domains S_1 and S_2 and must satisfy the boundary conditions.

In the case of the first boundary problem, when the surface forces on the contour are known, and if the body forces are neglected, it can be written in the general form

$$\varphi(t) + t\overline{\varphi'(t)} + \overline{\psi(t)} = \mathrm{i}\int_0^s (X_n + \mathrm{i}\,Y_n)\,\mathrm{d}s + C \qquad \text{on } L \tag{1}$$

where X_n and Y_n are components of the surface force on contour L in the x and y directions respectively, and C is an unknown complex constant. In the case of the second boundary problem, when the displacement state on the contour is prescribed, and if the body forces are neglected, it can be written in the general form

$$\chi\varphi(t) - t\overline{\varphi'(t)} - \overline{\psi(t)} = 2\mu(u_{nx} + \mathrm{i}u_{ny}) \qquad \text{on } L \tag{2}$$

where, in the case of plane stress, $\chi = (3-\nu)/(1+\nu)$, and, in the case of plane strain, $\chi = 3\text{–}4\nu$, ν is Poisson's ratio, $\mu = E/[2(1+\nu)]$, E is Young's modulus and u_{nx} and u_{ny} are displacements in the x and y directions respectively on L.

In the case where the shrink-fit contours L_1 and L_2 are unloaded, the only load is the displacement jump, δ, on the contact contour L_0. From equation (1) it can be written for the outer and inner contour as

$$\varphi_j(t_j) + t_j\overline{\varphi_j'(t_j)} + \overline{\psi_j(t_j)} = C_j \qquad \text{on } L_j\ (j = 1, 2) \tag{3}$$

where t_j are points on contour L_j (Fig. 1) and C_j are unknown complex constants. On the contact contour L_0, the same stress state must occur:

$$\varphi_1(t_0) + t_0\overline{\varphi_1'(t_0)} + \overline{\psi_1(t_0)} = \varphi_2(t_0) + t_0\overline{\varphi_2'(t_0)} + \overline{\psi_2(t_0)} \tag{4}$$

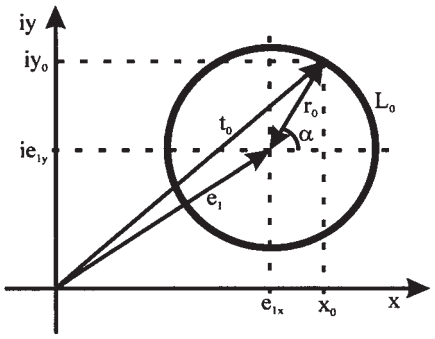

Fig. 2 Relationship between an angle α and the other geometry of a shrink-fit

where t_0 are points on contour L_0 (Fig. 1). Besides this, on the contact contour L_0 the difference in displacements of both members must be equal to the displacement jump δ. According to equation (2), it can be written as

$$\chi\varphi_2(t_0) - t_0\overline{\varphi_2'(t_0)} - \overline{\psi_2(t_0)} - \chi\varphi_1(t_0) + t_0\overline{\varphi_1'(t_0)} + \overline{\psi_1(t_0)} = 2\mu\delta\,\mathrm{e}^{\mathrm{i}\alpha} \tag{5}$$

The right-hand side of boundary condition (5) can be written in a different way according to Fig. 2:

$$\mathrm{e}^{\mathrm{i}\alpha} = \cos\alpha + \mathrm{i}\sin\alpha = \frac{x_0 + \mathrm{i}y_0 - (\mathrm{e}_{1x} + \mathrm{i}\mathrm{e}_{1y})}{r_0} = \frac{t_0 - e_1}{r_0} \tag{6}$$

Boundary conditions (3) to (5) must be satisfied by functions $\varphi_1(z)$, $\psi_1(z)$, $\varphi_2(z)$ and $\phi_2(z)$. Sherman reduced these four boundary conditions to two and wrote them in the form of the first boundary problem on contours L_1 and L_2.

Considering equations (4) to (6), and after some arrangement, it is possible to write

$$\varphi_2(t_0) = \varphi_1(t_0) + \frac{2\mu\delta(t_0 - e_1)}{(1+\chi)r_0} \tag{7}$$

If equation (7) is derivated with respect to t_0, conjugated, multiplied by t_0 and inserted into equations (4) and (5), it can be written as

$$\overline{\psi_2(t_0)} = \overline{\psi_1(t_0)} - \frac{2\mu\delta(2t_0 - e_1)}{(1+\chi)r_0} \tag{8}$$

Expression (8) is conjugated and, considering Fig. 2, can be written as

$$\psi_2(t_0) = \psi_1(t_0) - \frac{2\mu\delta}{(1+\chi)r_0}\left(\frac{2r_0^2}{t_0 - e_1} + \overline{e_1}\right) \tag{9}$$

In the next step, Sherman introduced two functions that are analytical in domain S_2. These functions are crucial for a solution of a shrink-fit problem in the elastic domain:

$$\varphi_*(z) = \varphi_2(z) \tag{10}$$

$$\psi_*(z) = \psi_2(z) + \frac{4\mu\delta r_0}{(1+\chi)(z - e_1)} \tag{11}$$

Expressions (10) and (11) are inserted into equations (7) and (9), so it is possible to write

$$\varphi_*(t_0) = \varphi_1(t_0) + \frac{2\mu\delta(t_0 - e_1)}{(1+\chi)r_0} \tag{12}$$

$$\psi_*(t_0) = \psi_1(t_0) - \frac{2\mu\delta\,\overline{e_1}}{(1+\chi)r_0} \tag{13}$$

Functions $\varphi_*(z)$ and $\psi_*(z)$ are analytical in domain S_2. From equations (12) and (13) it can be seen that they are analytical in domain S_1 too (analytical continuation of the complex function). This means that functions $\varphi_*(z)$ and $\psi_*(z)$ are analytical in the complete domain S, and it is possible to write

$$\varphi_*(z) = \varphi_1(z) + \frac{2\mu\delta(z - e_1)}{(1+\chi)r_0} \tag{14}$$

$$\psi_*(z) = \psi_1(z) - \frac{2\mu\delta\,\overline{e_1}}{(1+\chi)r_0} \tag{15}$$

Using functions $\varphi_*(z)$ and $\psi_*(z)$, boundary conditions (3) can now be expressed as

$$\varphi_*(t_1) + t_1\overline{\varphi_*'(t_1)} + \overline{\psi_*(t_1)} = \frac{4\mu\delta(t_1 - e_1)}{(1+\chi)r_0} + C_1 \quad \text{on } L_1 \tag{16}$$

$$\varphi_*(t_2) + t_2\overline{\varphi_*'(t_2)} + \overline{\psi_*(t_2)} = \frac{4\mu\delta r_0}{(1+\chi)(\overline{t_2} - \overline{e_1})} + C_2 \quad \text{on } L_2 \tag{17}$$

The problem of a shrink fit is written in the form of a first boundary problem, and boundary conditions (16) and (17) represent the basic equations that must be satisfied by functions $\varphi_*(z)$ and $\psi_*(z)$. Functions $\varphi_*(z)$ and $\psi_*(z)$ are sought in the form of Laurent's sums and, when they are known, functions $\varphi_1(z)$, $\psi_1(z)$, $\varphi_2(z)$ and $\psi_2(z)$ can be obtained from equations (10), (11), (14) and (15) respectively. The stress and displacement state in both members can finally be obtained from the well-known Kolosov's expressions

$$\begin{aligned} &\sigma_x + \sigma_y = 4\,\mathrm{Re}[\varphi_j'(z)], && j = 1,2\\ &\sigma_y - \sigma_x + 2\mathrm{i}\tau_{xy} = 2[\overline{z}\varphi_j''(z) + \psi_j'(z)], && j = 1,2\\ &2\mu(u_x - \mathrm{i}u_y) = \chi\overline{\varphi_j(z)} - \overline{z}\varphi_j'(z) - \psi_j(z), && j = 1,2 \end{aligned} \tag{18}$$

3 CONFORMAL MAPPING AND BOUNDARY CONDITIONS

The conformal mapping method is used in cases when domain S has an arbitrary shape and when it is very useful to be mapped to a circular domain Σ, where it is much easier to satisfy the boundary conditions. In the present case, the centric circular annulus domain Σ, which is defined by $\rho_1 \leqslant |\zeta| \leqslant \rho_2$ in complex plane $\zeta = \xi + \mathrm{i}\eta$, is conformally mapped into the domain of the eccentric circular annulus S in the complex plane $z = x + \mathrm{i}y$ (Fig. 3).

The bilinear conformal mapping function $z = \omega(\zeta)$ in this case is

$$\omega(\zeta) = \frac{\zeta}{1 - a\zeta}, \qquad a = \frac{e_0}{\sqrt{(r_1^2 - r_2^2)^2 - 2e_0^2(r_1^2 + r_2^2) + e_0^4}} \tag{19}$$

The inner radius ρ_1 and outer radius ρ_2 can be obtained from

$$\rho_1 = \frac{2r_1}{\sqrt{1 + 4a^2 r_1^2} + 1}, \qquad \rho_2 = \frac{2r_2}{\sqrt{1 + 4a^2 r_2^2} + 1} \tag{20}$$

The expression for e_1 (Fig. 3) is

$$e_1 = \overline{e_1} = \frac{a\rho_1^2}{1 - a^2\rho_1^2} \tag{21}$$

Boundary conditions (16) and (17) can be written on the mapped domain Σ after conjugation:

$$\overline{\varphi_*(\lambda_1)} + \frac{\overline{\omega(\lambda_1)}}{\omega'(\lambda_1)}\varphi_*'(\lambda_1) + \psi_*(\lambda_1) = \frac{4\mu\delta(\overline{\omega(\lambda_1)} - \overline{e_1})}{(1 + \chi)r_0} + \overline{C_1} \qquad \text{on } \gamma_1 \tag{22}$$

$$\overline{\varphi_*(\lambda_2)} + \frac{\overline{\omega(\lambda_2)}}{\omega'(\lambda_2)}\varphi_*'(\lambda_2) + \psi_*(\lambda_2) = \frac{4\mu\delta r_0}{(1 + \chi)[\omega(\lambda_2 - e_1)]} + \overline{C_2} \qquad \text{on } \gamma_2 \tag{23}$$

where λ_1 and λ_2 are points on contours γ_1 and γ_2. It is essential for further investigation to evaluate the right-hand side of equations (22) and (23). Let functions $f_1(\zeta)$ and $f_2(\zeta)$ be introduced, which can be written from equations (22) and (23) after using equations (19) and (21):

$$f_1(\zeta) = \frac{4\mu\delta(\overline{\omega(\zeta)} - \overline{e_1})}{(1 + \chi)r_0} = \frac{4\mu\delta(1 - a\zeta)}{(1 + \chi)r_0(1 - a^2\rho_1^2)(\zeta - a\rho_1^2)} \tag{24}$$

$$f_2(\zeta) = \frac{4\mu\delta r_0}{(1 + \chi)[\omega(\zeta) - e_1]} = \frac{4\mu\delta r_0(1 - a^2\rho_1^2)(1 - a\zeta)}{(1 + \chi)(\zeta - a\rho_1^2)} \tag{25}$$

It is possible to prove that functions $f_1(\zeta)$ and $f_2(\zeta)$ are always analytical in the domain Σ since the singular point $\zeta = a\rho_1^2$ always lies outside domain Σ (Fig. 3). This fact simplifies the mathematical treatment of this particular case. In the case of a shrink fit between two eccentric circular rings, functions $f_1(\zeta)$ and $f_2(\zeta)$ can, under certain circumstances, have singular points inside domain Σ. In the present paper, such difficulties will not be treated, though they can be solved [**10**].

For the finite, twofold connected domain Σ, functions $\varphi_*(\zeta)$ and $\psi_*(\zeta)$ can be written in the form of Laurent's sums:

$$\varphi_*(\zeta) = \sum_{k=-\infty}^{\infty} a_k\zeta^k, \qquad \psi_*(\zeta) = \sum_{k=-\infty}^{\infty} b_k\zeta^k \tag{26}$$

where a_k and b_k are unknown complex constants and can be determined from boundary conditions.

4 SOLUTION OF THE PROBLEM

In general, it is not possible to determine functions (26) in a closed and finite form. Sometimes [**11**, **12**], all constants from functions (26) can be determined, but, since they are infinite in number, the stress and displacement

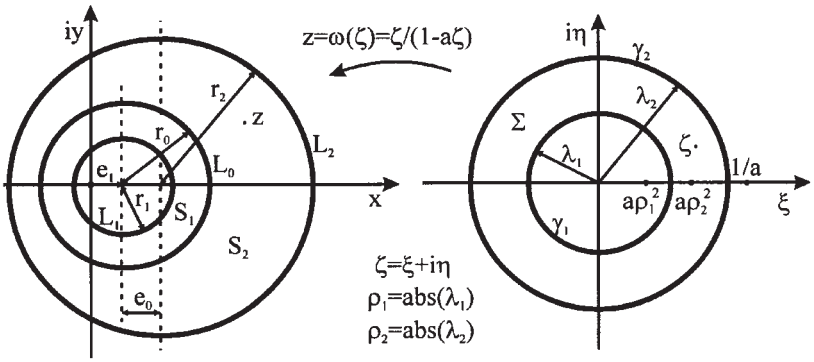

Fig. 3 Conformal mapping of the centric circular annulus to the eccentric one

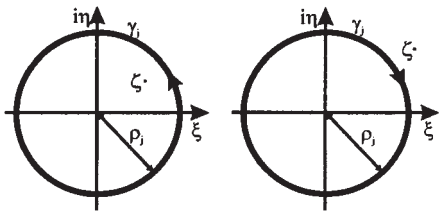

Fig. 4 Domains of integration of boundary conditions on contour γ_j, $j = 1, 2$

states cannot be expressed in a finite form. In the present case the function $\varphi_*(\zeta)$ is sought in a form that enables a closed and finite form, as proposed in reference [**13**]:

$$\varphi_*(\zeta) = \sum_{k=-\infty}^{\infty} a_k \zeta^k + \frac{A\zeta}{1 - a\zeta} \tag{27}$$

where A is an unknown real constant. When the x axis is the symmetrical axis (Fig. 3), all unknown constants are real:

$$C_1 = \overline{C_1}, \qquad C_2 = \overline{C_2}, \qquad a_k = \overline{a_k}, \qquad b_k = \overline{b_k},$$
$$A = \overline{A}$$

Let the boundary condition (22) be multiplied by

$$\frac{1}{2\pi \mathrm{i}} \frac{\mathrm{d}\lambda_1}{\lambda_1 - \zeta}$$

and let be it integrated on contour γ_1 around the domains $|\zeta| < \rho_1$ and $|\zeta| > \rho_1$ (Fig. 4), $j = 1$.

This method for solving the boundary conditions, when Cauchy-type integrals have to be solved, was introduced by Muskhelishvili [**7**]. The result of integration around both domains in Fig. 4, $j = 1$, can be written as

$$\psi_*(\zeta) = -\overline{\varphi_*}\left(\frac{\rho_1^2}{\zeta}\right) - \frac{\overline{\omega}(\rho_1^2/\zeta)}{\omega'(\zeta)} \varphi_*'(\zeta) + \frac{4\mu\delta\rho_1^2(1 - a\zeta)}{(1 + \chi)r_0(1 - a^2\rho_1^2)(\zeta - a\rho_1^2)} + C_1 \tag{28}$$

In a similar way, boundary condition (23) can be multiplied by

$$\frac{1}{2\pi \mathrm{i}} \frac{\mathrm{d}\lambda_2}{\lambda_2 - \zeta}$$

and integrated on contour γ_2 around the domains $|\zeta| < \rho_2$ and $|\zeta| > \rho_2$ (Fig. 4), $j = 2$. The result is

$$\psi_*(\zeta) = -\overline{\varphi_*}\left(\frac{\rho_2^2}{\zeta}\right) - \frac{\overline{\omega}(\rho_2^2/\zeta)}{\omega'(\zeta)} \varphi_*'(\zeta) + \frac{4\mu\delta r_0(1 - a^2\rho_1^2)(1 - a\zeta)}{(1 + \chi)(\zeta - a\rho_1^2)} + C_2 \tag{29}$$

Functions (28) and (29) can be equalized, so that only function $\varphi_*(\zeta)$ and constants C_1 and C_2 are unknown, and multiplied by $(\zeta - a\rho_1^2)(\zeta - a\rho_2^2)$. After some arrangement, it follows that

$$\begin{aligned} &2\rho_2^2 A\zeta + \sum_{k=-\infty}^{\infty} [(\rho_2^{2(2-k)} - \rho_1^{2(2-k)})a_{2-k} \\ &- a(\rho_1^2 + \rho_2^2)(\rho_2^{2(1-k)} - \rho_1^{2(1-k)})a_{1-k} \\ &+ a^2\rho_1^2\rho_2^2(\rho_2^{-2k} - \rho_1^{-2k})a_{-k}]\zeta^k + (\rho_2^2 - \rho_1^2) \\ &\times \sum_{k=-\infty}^{\infty} [ka_k - 2a(k-1)a_{k-1} + a^2(k-2)a_{k-2}]\zeta^k \\ &- 2\rho_1^2 A\zeta + (C_1 - C_2)[\zeta^2 - a(\rho_1^2 + \rho_2^2)\zeta + a^2\rho_1^2\rho_2^2] \\ &= \frac{4\mu\delta[\rho_1^2 - r_0^2(1 - a^2\rho_1^2)^2]}{(1 + \chi)r_0(1 - a^2\rho_1^2)} [a\zeta^2 - (1 + a^2\rho_2^2)\zeta + a\rho_2^2] \end{aligned} \tag{30}$$

Comparing the coefficients of ζ^k on both sides of equation (30), an infinite system of linear equations with an infinite number of unknowns (a_k; $k = \pm\infty$, A, C_1 and C_2) can be obtained. A suitable choice of function (27) enables equation (30) to be fulfilled for each k. Most of the constants a_k are zero, only a_{-1}, a_0 and a_1 are not, while one of the constants C_1 or C_2 cannot be determined, as is also known from the literature [**10**]. In the system of equations that emerges from equation (30), the constant a_0 does not appear and cannot be determined. A special name for constants a_0, C_1 and C_2 is additional constants, since they do not affect the stress state and the missing equation for determination of the displacement state is a condition of a single-valued solution [**7**]. For the present problem this condition connects a_0 and C_1 and will be presented later. The unknown constants from equation (30) are

$$\begin{aligned} a_1 &= \frac{4\mu\delta\rho_2^2[\rho_1^2 - r_0^2(1 - a^2\rho_1^2)^2]}{(1 + \chi)r_0(\rho_2^2 - \rho_1^2)} \\ &\quad \times [4a^2\rho_1^2\rho_2^2 - (\rho_1^2 + \rho_2^2)(1 + a^4\rho_1^2\rho_2^2)]^{-1} \\ a_{-1} &= a^2\rho_1^2\rho_2^2 a_1 \\ C_1 - C_2 &= \frac{a(\rho_2^2 - \rho_1^2)^2(1 - a^2\rho_2^2)}{\rho_2^2(1 - a^2\rho_1^2)} a_1 \\ A &= \frac{(\rho_1^2 - \rho_2^2)[a^2\rho_2^2(a^2\rho_2^2 - 2) + 1]}{2\rho_2^2} a_1 \end{aligned} \tag{31}$$

Functions $\varphi_*(\zeta)$ and $\psi_*(\zeta)$ can now be written as

$$\varphi_*(\zeta) = \frac{a_{-1}}{\zeta} + a_0 + a_1\zeta + \frac{A\zeta}{1 - a\zeta} \tag{32}$$

$$\psi_*(\zeta) = -\frac{a_{-1}\zeta}{\rho_1^2} - a_0 - \frac{a_1\rho_1^2}{\zeta} - \frac{\rho_1^2(1 - a\zeta)^2}{\zeta - a\rho_1^2}\left(a_1 - \frac{a_{-1}}{\zeta^2}\right) - \frac{2A\rho_1^2}{\zeta - a\rho_1^2} + \frac{4\mu\delta(1 - a\zeta)e_1}{(1 + \chi)r_0 a(\zeta - a\rho_1^2)} + C_1 \tag{33}$$

In order to determine function $\psi_*(\zeta)$, it is not necessary to know constants b_k from the second of functions (26), since equations (28) or (29) can be used instead. It turns out to be better to use equation (28) since $\overline{\omega}(\rho_2^2/\zeta)$ in equation (29) can have, at great values of eccentricities e_0, a singular point $\zeta = a\rho_2^2$ inside domain Σ (Fig. 3). The other three possible singular points $\zeta = 0$, $\zeta = 1/a$ and $\zeta = a\rho_1^2$ are never inside domain Σ. In this way, expressions (32) and (33) are analytical in domain Σ, as claimed by Sherman's theory.

A condition of the single-valued solution of the plane elasticity problem has the following general form:

$$\chi a_0 - b_0 = 0$$

In the present case it can be obtained from expressions (32) and (33) in the following form:

$$(\chi+1)a_0 - C_1 = a\rho_1^2(2 - a^2\rho_1^2)a_1 - \frac{4\mu\delta a\rho_1^2 e_1}{(1+\chi)r_0} \tag{34}$$

In the present case, expression (34) appears in the equation for determination of the displacement state [equation (18)]. In this way, not only the stress state but also the displacement state is determined, even though one of the constants a_0, C_1 or C_2 cannot be determined.

Using function (19), $\varphi_*(z)$ and $\psi_*(z)$ can be determined from expressions (32) and (33), and then $\varphi_1(z)$, $\psi_1(z)$, $\varphi_2(z)$ and $\psi_2(z)$ can be determined from expressions (14), (15), (10) and (11) respectively. The stress and displacement states in a circular centric annulus can finally be determined using $\varphi_1(z)$ and $\psi_1(z)$ in expressions (18):

$$\sigma_x + \sigma_y = 4\,\mathrm{Re}\left[-\frac{a_{-1}}{z^2} + \frac{a_1}{(1+az)^2} + A - \frac{2\mu\delta}{(1+\chi)r_0}\right]$$

$$\sigma_y - \sigma_x + 2\mathrm{i}\tau_{xy} = 2\left\{\frac{2a_{-1}\bar{z}}{z^3} - \frac{2aa_1\bar{z}}{(1+az)^3} - \frac{a_{-1}}{\rho_1^2(1+az)^2} + \frac{a_1\rho_1^2}{z^2} + \frac{\rho_1^2(1-a^2\rho_1^2)}{[(1-a^2\rho_1^2)z - a\rho_1^2]^2}\left[\frac{a_1}{1+az} + (1+az)\left(2A - \frac{a_{-1}}{z^2}\right) - \frac{4\mu\delta}{(1+\chi)r_0(1-a^2\rho_1^2)}\right] + \frac{\rho_1^2}{(1-a^2\rho_1^2)z - a\rho_1^2}\left[\frac{aa_1}{(1+az)^2} - a\left(2A - \frac{a_{-1}}{z^2}\right) - \frac{2(1+az)a_{-1}}{z^3}\right]\right\}$$

$$\begin{aligned}2\mu(u_x - \mathrm{i}u_y) = {}& \chi\left[\left(a + \frac{1}{\bar{z}}\right)a_{-1} + \frac{a_1\bar{z}}{1+a\bar{z}}\right] + (\chi-1)\left[A\bar{z} - \frac{2\mu\delta}{(1+\chi)r_0}\left(\bar{z} - \frac{a\rho_1^2}{1-a^2\rho_1^2}\right)\right] \\ & + \frac{a_{-1}\bar{z}}{z^2} - \frac{a_1\bar{z}}{(1+az)^2} + \frac{a_{-1}z}{\rho_1^2(1+az)} + \rho_1^2\left(a + \frac{1}{z}\right)a_1 + \frac{\rho_1^2}{(1-a^2\rho_1^2)z - a\rho_1^2} \\ & \times\left[\frac{a_1}{1+az} + (1+az)\left(2A - \frac{a_{-1}}{z^2}\right) - \frac{4\mu\delta}{(1+\chi)r_0(1-a^2\rho_1^2)}\right] + (\chi+1)a_0 - C_1\end{aligned} \tag{35}$$

The stress and displacement state in a circular eccentric annulus are determined from expressions (18) using $\varphi_2(z)$ and $\phi_2(z)$:

$$\sigma_x + \sigma_y = 4\,\mathrm{Re}\left[-\frac{a_{-1}}{z^2} + \frac{a_1}{(1+az)^2} + A\right]$$

$$\begin{aligned}\sigma_y - \sigma_x + 2\mathrm{i}\tau_{xy} = {}& 2\left(\frac{2a_{-1}\bar{z}}{z^3} - \frac{2aa_1\bar{z}}{(1+az)^3} - \frac{a_{-1}}{\rho_1^2(1+az)^2} + \frac{a_1\rho_1^2}{z^2} + \frac{\rho_1^2(1-a^2\rho_1^2)}{[(1-a^2\rho_1^2)z - a\rho_1^2]^2}\right. \\ & \times\left\{\frac{a_1}{1+az} + (1+az)\left(2A - \frac{a_{-1}}{z^2}\right) - \frac{4\mu\delta}{1+\chi}\left[\frac{1}{r_0(1-a^2\rho_1^2)} - r_0\left(\frac{1}{\rho_1^2} - a^2\right)\right]\right\} \\ & \left. + \frac{\rho_1^2}{(1-a^2\rho_1^2)z - a\rho_1^2}\left[\frac{aa_1}{(1+az)^2} - a\left(2A - \frac{a_{-1}}{z^2}\right) - \frac{2(1+az)a_{-1}}{z^3}\right]\right)\end{aligned}$$

$$\begin{aligned}2\mu(u_x - \mathrm{i}u_y) = {}& \chi\left[\left(a + \frac{1}{\bar{z}}\right)a_{-1} + \frac{a_1\bar{z}}{1+a\bar{z}} + A\bar{z}\right] - \bar{z}\left(A - \frac{a_{-1}}{z^2} + \frac{a_1}{(1+az)^2}\right) + \frac{a_{-1}z}{\rho_1^2(1+az)} + \rho_1^2\left(a + \frac{1}{z}\right)a_1 \\ & + \frac{\rho_1^2}{(1-a^2\rho_1^2)z - a\rho_1^2}\left\{\frac{a_1}{1+az} + (1+az)\left(2A - \frac{a_{-1}}{z^2}\right) - \frac{4\mu\delta}{1+\chi}\left[\frac{1}{r_0(1-a^2\rho_1^2)} - \left(\frac{1}{\rho_1^2} - a^2\right)r_0\right]\right\} \\ & + (\chi+1)a_0 - C_1\end{aligned} \tag{36}$$

Solving expressions (35) and (36) is mathematically simple but cumbersome and, for this task, computer programs where complex numbers can be used are available (e.g. Fortran). If eccentricity e_0 is zero, then expressions (35) and (36) are simplified and represent the solution of a shrink fit between two centric circular rings, which is well known.

5 NUMERICAL EXAMPLES

It is advisable to introduce dimensionless ratios into equations (31) to (36):

$$k_1 = \frac{r_1}{r_0}, \quad k_2 = \frac{r_2}{r_0}, \quad k_3 = \frac{e_0}{r_0}, \quad k_4 = \frac{\delta}{r_0}, \quad z_0 = \frac{z}{r_0}$$

In all numerical examples, a plane stress state is assumed, $\chi = (3-\nu)/(1+\nu)$. Firstly, elements of the stress tensors in shrink-fitted steel members are determined. The Young's modulus and Poisson's ratio for both members are the same: $E = 210\,\text{GPa}$ and $\nu = 0.3$. The geometry is: $k_1 = 2/3$, $k_2 = 2$, $k_3 = 2/3$ and $k_4 = 0.001$. Stresses at some points in both members are shown in Fig. 5.

For practical use it is more interesting to calculate the effective stress, σ_E, which allows comparison with a uniaxial stress state. It can be calculated according to Huber that

$$\sigma_E = \sqrt{\sigma_x^2 + \sigma_y^2 - \sigma_x\sigma_y + 3\tau_{xy}^2} \tag{37}$$

Figure 6 shows the relationship between $k_1 = r_1/r_0$ and the maximum effective stress σ_E in both members. At $k_1 = 0.569$, the maximum effective stresses σ_E in both members are equal. In the centric annulus the critical point is A, and in the eccentric annulus it is B. Figure 7 presents the relationship between $k_4 = \delta/r_0$ and the maximum effective stress σ_E in both members. As before, the critical points are A in the centric annulus and B in the eccentric annulus. It can also be seen that the stress–strain state in both members is in the elastic domain, since the relationship between the effective stress σ_E and $k_4 = \delta/r_0$ is linear.

Figure 8 shows the relationship between $k_3 = e_0/r_0$ and $k_4 = \delta/r_0$ under the condition that the maximum effective stress σ_E in the shrink-fit assembly is equal to the yield stress σ_Y, which, for mild structural steel (0.17 per cent carbon), is equal to $\sigma_Y = \sigma_E = 245\,\text{MPa}$. At most values of eccentricity, A is the critical point for the centric annulus. Only at extreme values of eccentricity, $k_3 \geqslant 2.753$, does B become the critical point of the eccentric annulus. However, such values of eccentricity are interesting only theoretically. The allowable displacement jump is almost constant in the range of eccentricities that are practically important and even increases in the range $0.6 \leqslant k_3 \leqslant 2.753$.

Another point of interest is to examine the progress of change in the value of torque M_t, which can be borne by the shrink-fit assembly and still prevent slip between the rings, and eccentricity e_0. A shrink-fit assembly bears torque M_t with friction and can be calculated from the equation

$$M_t = 2r_0^2 h\mu_S \int_0^\pi \sigma_n \, d\alpha \tag{38}$$

where h is the width of the inner and outer member, or of the shrink-fit assembly, μ_S is the coefficient of static

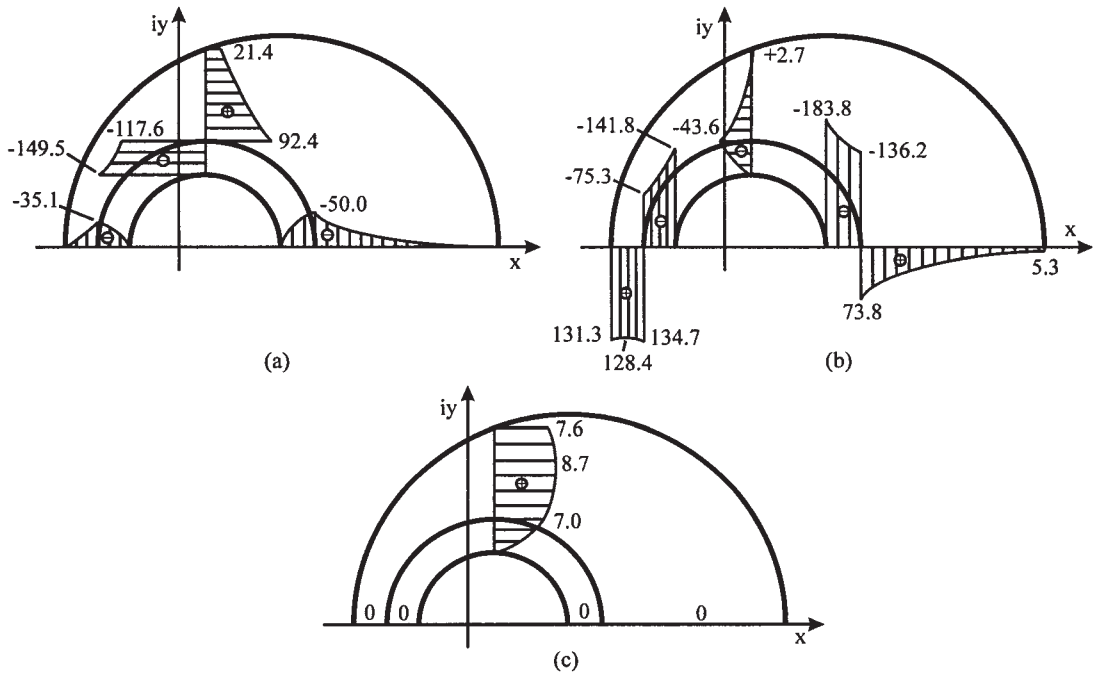

Fig. 5 Stresses in both members: (a) normal stress σ_x (MPa); (b) normal stress σ_y (MPa); (c) shear stress τ_{xy} (MPa)

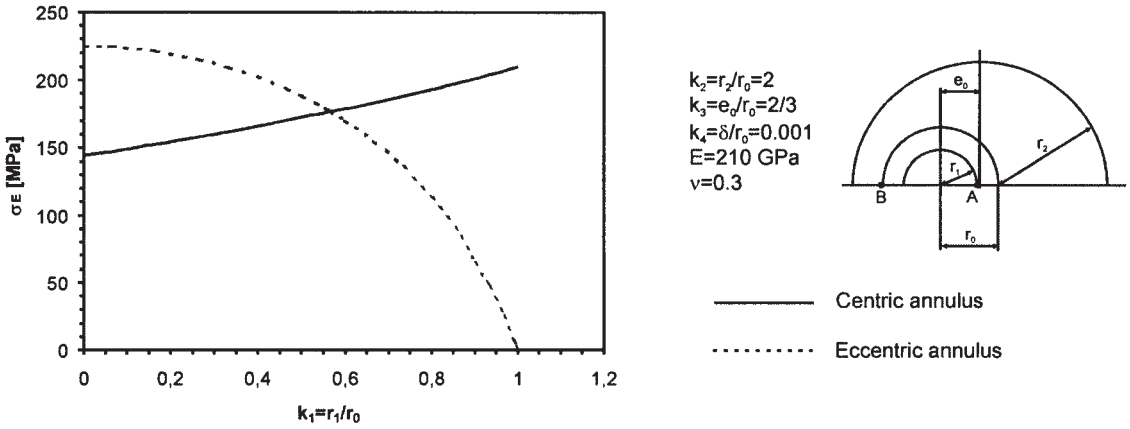

Fig. 6 Maximum effective stress σ_E versus $k_1 = r_1/r_0$

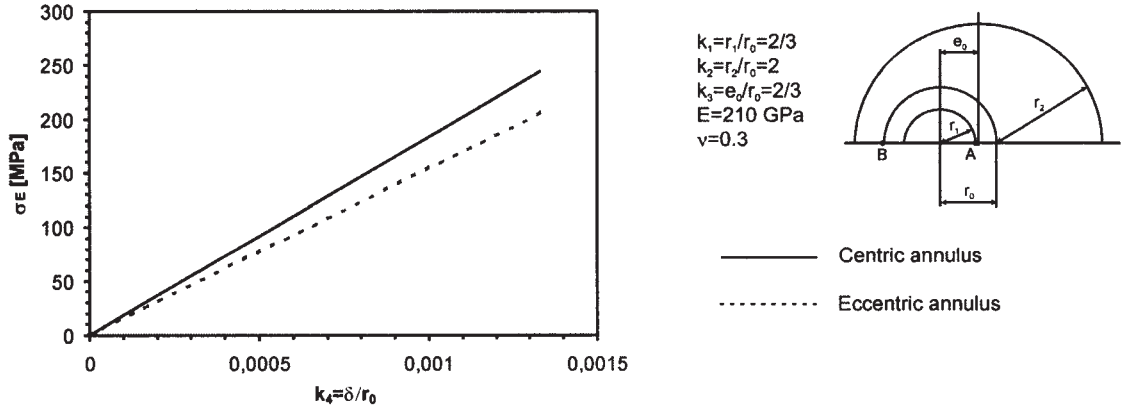

Fig. 7 Maximum effective stress σ_E versus $k_4 = \delta/r_0$

friction between the rings, σ_n is the normal stress on contact contour L_0 and α is the angle in Fig. 2. Stress σ_n can be calculated from the equation

$$\sigma_n = \frac{\sigma_x + \sigma_y}{2} + \frac{\sigma_x - \sigma_y}{2}\cos(2\alpha) + \tau_{xy}\sin(2\alpha) \qquad (39)$$

There is also shear stress τ_n on the contact contour L_0, which in general also affects the value of torque M_t. However, in the present case, because of the symmetry, its overall contribution is zero. The elements of the stress tensor in formula (39) can be calculated from expression (35).

Figure 9 shows torque M_t versus $k_3 = e_0/r_0$ for the same example as in Fig. 8. The value of $k_4 = \delta/r_0$ is chosen so that at the critical point the maximum effective stress σ_E is equal to the yield stress σ_Y.

The capacity of a shrink-fit assembly to avoid slip between rings decreases as eccentricity increases. In the

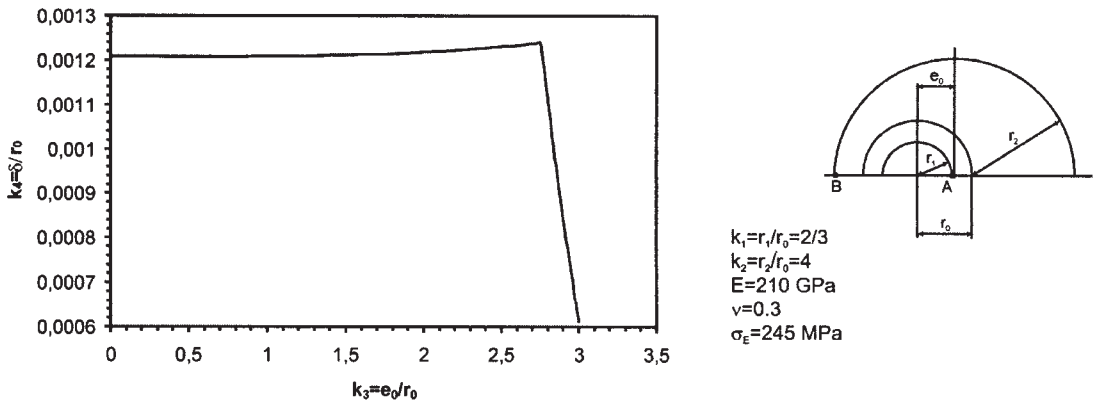

Fig. 8 Relationship between $k_4 = \delta/r_0$ and $k_3 = e_0/r_0$, if the effective stress σ_E is equal to the yield stress σ_Y

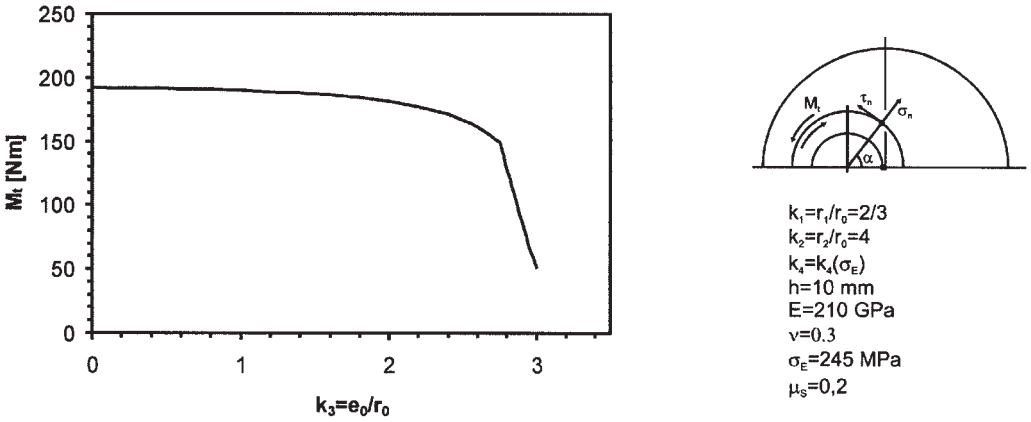

Fig. 9 Torque M_t which can be borne by a shrink-fit assembly and still avoid slip versus $k_3 = e_0/r_0$

range $k_3 \leqslant 1.65$ this decrease is much slower than at greater values of k_3. As in Fig. 8, the capacity to avoid slip decreases rapidly when $k_3 \geqslant 2.753$.

A plane stress state is assumed in all examples presented here. Similar results can be obtained in the case of a plane strain state.

6 CONCLUSIONS

On the basis of a suitable choice of function $\varphi_*(\zeta)$, the closed and finite-form solution of a shrink fit between an eccentric and a centric circular annulus in the elastic domain has been presented.

On the basis of numerical examples it can be concluded that eccentricity does not affect greatly the maximum effective stress in a shrink-fit assembly, except at greatest values of eccentricities. The value of the torque that can be borne by a shrink-fit assembly and still avoid slip decreases increasingly rapidly with increasing eccentricity.

One possible practical application of this theory is in the case of shrink-fitted 'snail-cams'.

In future, it would be useful to treat this problem also in the elastoplastic domain. It can be seen that, even at relatively small values of displacement jump, the maximum effective stress can easily exceed the yield stress of a given material.

REFERENCES

1 **Stagni, L.** Elastic field perturbation by misfitting ring inclusion. *Mechanics Res. Commun.*, 2003, **30**, 39–44.

2 **Stagni, L.** Elastic analysis of a multilayered cylindrical fiber with eigenstrains. *Int. J. Engng Sci.*, 2001, **39**, 641–653.

3 **Urriolagoitia Sosa, G., Hills, D. A.** and **Sackfield, A.** A shrink-fit peg subject to bending and shearing forces. *J. Strain Analysis*, 1999, **34**(1), 23–29.

4 **Mugadu, A.,** and **Hills, D. A.** A shrink-fitted peg subjected to a tensile load. *Int. J. Mech. Sci.*, 2001, **43**, 1629–1641.

5 **Sackfield, A., Barber, J. R., Hills, D. A.** and **Truman, C. E.** A shrink-fit shaft subject to torsion. *Eur. J. Mechanics A/Solids*, 2002, **21**, 73–84.

6 **Kolosov, G. V.** On an application of complex function theory to a plane problem of the mathematical theory of elasticity (in Russian). PhD thesis, Dorpat University, Estonia, 1909.

7 **Muskhelishvili, N. I.** *Some Basic Problems of the Mathematical Theory of Elasticity*, 1953 (Noordhoof, Groningen, The Netherlands).

8 **Sherman, D. I.** The static plane problem of the theory of elasticity for isotropic non-homogeneous media (in Russian). *Trudy Seismologichesk. Inst. Akad. Nauk SSSR*, 1938, **86**, 1–50.

9 **Sherman, D. I.** 1940. On a problem of the theory of elasticity (in Russian). *Dokl. Akad. Nauk SSSR*, 1940, **27**(9), 907–910.

10 **Ugodchikov, A. G., Dlugach, M. I.** and **Stepanov, A. E.** *Computational Methods in Boundary Value Problems of the Plane Theory of Elasticity* (in Russian) , 1970 (Vishcha Shkola, Moscow, USSR).

11 **Batista, M.** and **Usenik J.** Stresses in a circular ring under two forces acting along a diameter. *J. Strain Analysis*, 1996, **31**(1), 75–78.

12 **Batista, M.** Stresses in a confocal elliptic ring subject to uniform pressure. *J. Strain Analysis*, 1999, **34**(3), 217–221.

13 **Batista, M. and Kosel, F.** Elastic state in eccentric ring under uniform normal load. *Z. Angew. Math. Mech.*, 1995, **75**(SII), 453–454.